IMAGE ENHANCEMENT NETWORK TRAINED BY USING HDR IMAGES

Yuma Kinoshita and Hitoshi Kiya

Tokyo Metropolitan University, Tokyo, Japan

ABSTRACT

In this paper, a novel image enhancement network is proposed, where HDR images are used for generating training data for our network. Most of conventional image enhancement methods, including Retinex based methods, do not take into account restoring lost pixel values caused by clipping and quantizing. In addition, recently proposed CNN based methods still have a limited scope of application or a limited performance, due to network architectures. In contrast, the proposed method have a higher performance and a simpler network architecture than existing CNN based methods. Moreover, the proposed method enables us to restore lost pixel values. Experimental results show that the proposed method can provides higher-quality images than conventional image enhancement methods including a CNN based method, in terms of TMQI and NIQE.

Index Terms— Image enhancement, High dynamic range images, Deep learning, Convolutional neural networks

1. INTRODUCTION

The low dynamic range (LDR) of modern digital cameras is a major factor preventing cameras from capturing images as well as human vision. This is due to the limited dynamic range that imaging sensors have. This limit results in low contrast in images taken by digital cameras. The purpose of enhancing images is to show hidden details in such images.

Various kinds of research on single-image enhancement have so far been reported [1–6]. Most of image enhancement methods can be divided into two methods: histogram equalization (HE) based methods and Retinex-based methods. However, both HE- and Retinex-based methods cannot restore lost pixel values due to quantizing and clipping. For this reason, a few image enhancement method based on convolutional neural networks (CNNs) have recently been developed [7, 8].

CNN based methods can solve the problem that traditional methods have, but there are still some issues. Chen's method [7] is only applicable to raw images, so existing RGB color images cannot be enhanced. Yang's method [8] generates intermediate high dynamic range (HDR) images from

RGB images, and then high-quality LDR images are produced. However, generating HDR images from single images is an outstanding problem yet, as well-known [9, 10]. For this reason, the performance of Yang's method is limited by the quality of intermediate HDR images. Furthermore, it is difficult to collect numerous training data with sufficient quality due to the narrow dynamic range of digital cameras.

Thus, in this paper, we propose a novel image enhancement network trained by using HDR images. The proposed method can restore lost pixel values without generating intermediate HDR images. For training of a CNN used in the proposed method, we utilize existing HDR images. The use of HDR images makes it easy to collect training data for the CNN used in the proposed method. Specifically, both input images and target images are mapped from HDR images by tone mapping operations [11,12]. Because HDR images have much information that LDR images captured with cameras do not have, target LDR images mapped from HDR ones have better quality than that LDR ones directly captured with cameras.

We evaluate the effectiveness of the proposed image enhancement network in terms of the quality of enhanced images in a number of simulations, where TMQI and NIQE are utilized as quality metrics. Experimental results show that the proposed method can restore lost pixel values. In addition, the proposed method outperforms state-of-the-art contrast enhancement methods in terms of both TMQI and NIQE.

2. RELATED WORK

Here, we summarize conventional image enhancement methods including state-of-the-art ones, and recapitulate tone mapping methods used for the proposed method.

2.1. Image enhancement

So far, a lot of image enhancement methods have been studied [1–6]. Among methods for enhancing images, HE has received the most attention because of its intuitive implementation quality and high efficiency. It aims to derive a mapping function such that the entropy of a distribution of output luminance values can be maximized, but HE often causes overenhancement. To avoid the over-enhancement, numerous improved methods based on HE have also been developed [1,2]. Another way for enhancing images is to use the Retinex theory [13]. Retinex-based methods [3, 4] decompose images into reflectance and illumination, and then enhance images

This work was supported by JSPS KAKENHI Grant Number JP18J20326.

by manipulating illumination. However, these methods without CNNs cannot restore lost pixel values due to clipping and

Recently, a few CNN based methods were proposed [7,8]. Chen's method [7] provides high-quality RGB images from single raw images taken under low-light conditions, but this method cannot be applied to RGB color images. Yang's et al. [8] proposed a method for enhancing RGB images by using two CNNs. This method generates intermediate high dynamic range (HDR) images from input RGB images, and then high-quality LDR images are produced. However, generating HDR images from single images is an outstanding problem yet, as well-known [9, 10]. For this reason, the performance of Yang's method is limited by the quality of intermediate HDR images. In addition, collecting training data with sufficient quality is problematic due to the narrow dynamic range of digital cameras.

2.2. Tone mapping

Tone mapping is an operation that generates an LDR image from an HDR image [11, 12]. LDR images mapped from HDR images generally have higher quality than LDR ones directly captured with cameras. This is because HDR images have much information that LDR images captured with cameras do not have.

Here, we summarize Reinhard's global operator which is one of typical tone mapping methods, as an example [11]. Under the use of the operator, each pixel value in LDR image I is calculated from HDR image E by

$$I_{i,j} = \hat{f}(X_{i,j}),\tag{1}$$

$$\hat{f}(X_{i,j}) = \frac{X_{i,j}}{1+X_{i,j}}, \tag{2}$$
 where (i,j) denotes a pixel and $X_{i,j}$ is given by using two

parameters a and G(E) as

$$X_{i,j} = \frac{a}{G(E)} E_{i,j}.$$
 (3)

In Reinhard's global operator, two parameters a and G(E)are used. $a \in [0,1]$ determines brightness of an output LDR image I and G(E) is the geometric mean of E. G(E) is calculated as

$$G(E) = \exp\left(\frac{1}{|\mathbf{P}|} \sum_{(i,j)\in\mathbf{P}} \log\left(\max\left(E_{i,j},\epsilon\right)\right)\right), \quad (4)$$

where P is the set of all pixels and ϵ is a small value to avoid singularities at $E_{i,j} = 0$.

Tone mapping operations enables us not only to generate high-quality LDR images but also to simulate a digital camera, i.e., a virtual camera. For this reason, the proposed image enhancement network utilize LDR images mapped from HDR images as training data.

3. PROPOSED IMAGE ENHANCEMENT NETWORK

Figure 1 shows an overview of our training procedure and predicting procedure. In the training, all input LDR images x and target LDR images y are generated from HDR images by

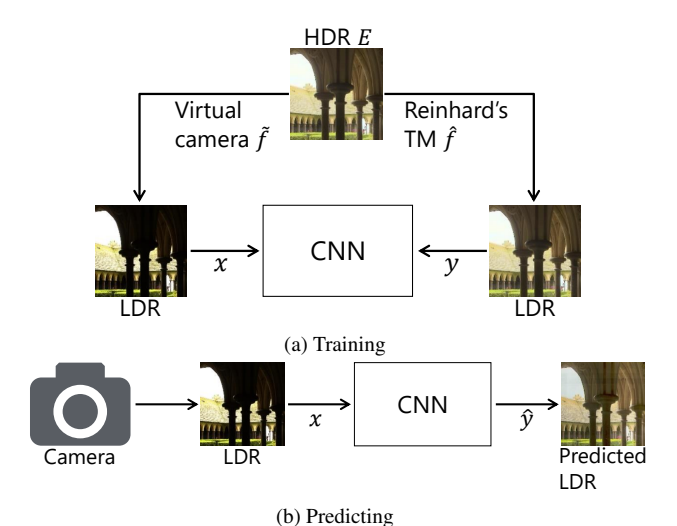


Fig. 1. Proposed image enhancement method Output image Max pool Transposed conv - + Concatenation Conv

Fig. 2. Network architecture. Each box denotes multichannel feature map produced by each layer (or block). Number of channels is denoted on top or bottom of each box. Resolution of feature map is provided at left edge of box.

a virtual camera [9] and Reinhard's global operator, respectively. This enables us not only to generate high-quality target images, but also to easily collect training data. In addition, the proposed method has a simpler network architecture than the conventional method [8] because the proposed method do not generate intermediate HDR images.

After the training, various LDR images are applied to the proposed network as input images, and then high-quality LDR images are generated by the network. Detailed training conditions will be shown in 3.2.

3.1. Network architecture

Figure 2 shows the network architecture of the CNN used in the proposed method. The CNN is designed on the basis of U-Net [14]. The input of this CNN is a 24-bit color LDR image with a size of 512×512 pixels.

Each convolutional block consists of two convolutional

layers, in which the number of filters K is commonly the same. From the first block to the last block, the numbers are given as K=32,64,128,256,512,1024,512,256,128,64, and 32, where all filters in convolutional blocks have a size of 3×3 . Max pooling layers with a kernel size of 2×2 and a stride of 2 are utilized for image downsampling.

For image upsampling, transposed convolutional layers with a stride of 2 and a filter size of 4 are used in the proposed method. From the first transposed convolutional layer to the last one, the numbers of filters are K=512,256,128,64, and 32, respectively. Finally, an output LDR image is produced by a convolutional layer which has three filters with a size of 3×3 .

The rectified linear unit (ReLU) activation function [15] is employed for all convolutional layers and transposed convolutional ones except the final convolutional layer. Further, batch normalization [16] is applied to outputs of ReLU functions after convolutional layers. The activation function of the final layer is a sigmoid function.

3.2. Training

A lot of LDR images x taken under various conditions and corresponding LDR ones y with high-quality are needed for training the CNN in the proposed method. However, collecting these images with a sufficient amount is difficult. We therefore utilize HDR images E to generate both input LDR images E and target LDR images E by using a virtual camera [9] and Reinhard's global operator, respectively. For training, total 978 HDR images was collected from online available databases [17–22].

A training procedure of our CNN is shown as follows.

- Select eight HDR images from 978 HDR images at random.
- ii Generate total eight couples of input LDR image x and target LDR one y from each of the eight HDR ones. Each couple is generated according to the following steps.
 - (a) Crop an HDR image E to an image patch \tilde{E} with $N \times N$ pixels. The size N is given as a product of a uniform random number in range [0.2, 0.6] and the length of a short side of E. In addition, the position of the patch in the HDR image E is also determined at random.
 - (b) Resize \tilde{E} to 512×512 pixels.
 - (c) Flip \tilde{E} upside down with probability 0.5.
 - (d) Flip \tilde{E} left and right with probability 0.5.
 - (e) Calculate exposure X from \tilde{E} by $X_{i,j} = \Delta t \cdot \tilde{E}$, where shutter speed Δt is calculated as $\Delta t = 0.18 \cdot 2^v/G(\tilde{E})$ as in [11] by using a uniform random number v in range [-4,4].
 - (f) Generate an input LDR image x from X by a virtual camera \tilde{f} , as

$$x = \tilde{f}(X) = \min\left((1+\eta)\frac{X^{\gamma}}{X^{\gamma}+\eta}, 1\right), \quad (5)$$
where η and γ are random numbers that follow nor-

- mal distributions with mean 0.6 and variance 0.1 and with mean 0.9 and variance 0.1, respectively.
- (g) Generate a target LDR image y from \tilde{E} by Reinhard's global operator (see eq. (1) to eq. (4)) with parameter a = 0.18, where the parameter maps the average luminance of y to the middle gray [11].
- iii Predict eight LDR images \hat{y} from eight input LDR images x by the CNN.
- Evaluate errors between predicted images \hat{y} and target images y by using the mean squared error.
- v Update filter weights ω and biases b in the CNN by back-propagation.

Note that steps ii(f) and ii(g) are applied to luminance of \tilde{E} , and then RGB pixel values of x and y are obtained so that ratios of RGB values of LDR images are equal to those of HDR images.

In our experiments, the CNN was trained with 5000 epochs, where the above procedure was repeated 122 times in each epoch. In addition, each HDR image had only one chance to be selected, in step i in each epoch. He's method [23] was used for initialization of the CNN In addition, Adam optimizer [24] was utilized for optimization, where parameters in Adam were set as $\alpha=0.002, \beta_1=0.5$ and $\beta_2=0.999$.

4. SIMULATION

We evaluated the effectiveness of the proposed method by using two objective quality metrics.

4.1. Simulation conditions

In this experiment, test LDR images was generated from eight HDR images which were not used for training, according to steps from ii(a) to ii(f).

The quality of LDR images \hat{y} generated by the proposed method was evaluated by two objective quality metrics: the tone mapped image quality index (TMQI) [25] and the naturalness image quality evaluator (NIQE) [26], where original HDR image \tilde{E} was utilized as a reference for TMQI.

The proposed method is compared with four conventional methods: histogram equalization (HE), contrast-accumulated histogram equalization (CACHE) [2], simultaneous reflectance and illumination estimation (SRIE) [4], and deep reciprocating HDR transformation ¹ (DRHT) [8], where SRIE is a Retinex-based method and DRHT is a CNN-based one.

4.2. Results

Figures 3 and 4 show examples of HDR images generated by the five methods.

From Fig. 3, it is confirmed that the proposed method produced an higher-quality image which clearly represent dark areas in the image. The image generated by DRHT is still unclear due to the difficulty of generating an intermediate HDR

 $^{^1\}mbox{An}$ approximate implementation at https://github.com/ybsong00/DRHT was utilized

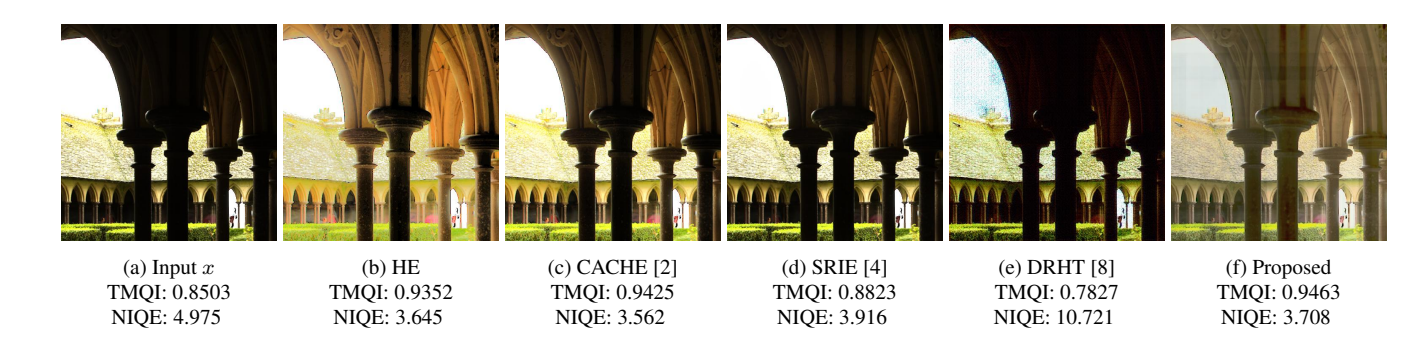


Fig. 3. Experimental Results (Image 5) (c) CACHE [2] (d) SRIE [4] (e) DRHT [8] (a) Input x(b) HE (f) Proposed TMQI: 0.4308 TMOI: 0.8705 TMQI: 0.7537 TMQI: 0.4830 TMQI: 0.4027 TMQI: 0.5491 NIQE: 5.462 NIQE: 5.949 NIQE: 4.883 NIQE: 4.656 NIQE: 17.783 NIQE: 3.879

Fig. 4. Experimental Results (Image 7)

Table 1. TMQI scores							Table 2. NIQE scores							
Input	HE	CACHE [2]	SRIE [4]	DRHT [8]	Proposed			Input	HE	CACHE [2]	SRIE [4]	DRHT [8]	Proposed	
.7858	0.8469	0.7427	0.7710	0.7682	0.9124	•	Image 1	4.055	4.267	3.552	4.076	9.901	4.218	
.6624	0.7422	0.6852	0.6624	0.6543	0.8870		Image 2	4.740	5.064	4.919	4.723	12.145	2.870	
.9394	0.9590	0.8580	0.8712	0.8809	0.8687		Image 3	4.609	5.221	4.703	4.605	8.720	3.951	
.6069	0.9215	0.9028	0.7441	0.5104	0.7693		Image 4	6.754	6.918	4.904	4.191	17.873	4.127	
.8503	0.9352	0.9425	0.8823	0.7827	0.9463		Image 5	4.975	3.645	3.562	3.916	10.721	3.708	
.8178	0.8502	0.9034	0.8808	0.7772	0.9104		Image 6	5.118	4.556	4.698	4.920	10.523	4.220	
.4308	0.8705	0.7537	0.4830	0.4027	0.5491		Image 7	5.462	5.949	4.883	4.656	17.783	3.879	
.7468	0.9031	0.8044	0.7461	0.6131	0.5969	-	Image 8	5.803	5.869	4.289	5.775	13.515	4.112	
	7858 6624 9394 6069 8503 8178 4308	nput HE 7858 0.8469 6624 0.7422 9394 0.9590 6069 0.9215 8503 0.9352 8178 0.8502 4308 0.8705	nput HE CACHE [2] 7858 0.8469 0.7427 0.6852 6624 0.7422 0.6852 0.8580 6069 0.9215 0.9028 0.9028 8503 0.9352 0.9425 0.9034 4308 0.8705 0.7537	nput HE CACHE [2] SRIE [4] 7858 0.8469 0.7427 0.7710 6624 0.7422 0.6852 0.6624 9394 0.9590 0.8580 0.8712 6069 0.9215 0.9028 0.7441 8503 0.9352 0.9425 0.8823 8178 0.8502 0.9034 0.8808 4308 0.8705 0.7537 0.4830	nput HE CACHE [2] SRIE [4] DRHT [8] 7858 0.8469 0.7427 0.7710 0.7682 0.6624 0.7422 0.6852 0.6624 0.6543 9394 0.9590 0.8580 0.8712 0.8809 0.8712 0.8809 6609 0.9215 0.9028 0.7441 0.5104 0.5104 8503 0.9352 0.9425 0.8823 0.7827 8178 0.8502 0.9034 0.8808 0.7772 4308 0.8705 0.7537 0.4830 0.4027	nput HE CACHE [2] SRIE [4] DRHT [8] Proposed 7858 0.8469 0.7427 0.7710 0.7682 0.9124 0.6624 0.6543 0.8870 6624 0.7422 0.6852 0.6624 0.6543 0.8870 0.8580 0.8712 0.8809 0.8687 6069 0.9215 0.9028 0.7441 0.5104 0.7693 0.9352 0.9425 0.8823 0.7827 0.9463 8178 0.8502 0.9034 0.8808 0.7772 0.9104 4308 0.8705 0.7537 0.4830 0.4027 0.5491	Nput HE CACHE [2] SRIE [4] DRHT [8] Proposed	Nput HE CACHE [2] SRIE [4] DRHT [8] Proposed	Input HE CACHE [2] SRIE [4] DRHT [8] Proposed Image 1 4.055	Input HE CACHE [2] SRIE [4] DRHT [8] Proposed Input HE T858 0.8469 0.7427 0.7710 0.7682 0.9124 Image 1 4.055 4.267 0.9394 0.9590 0.8580 0.8712 0.8809 0.8687 Image 2 4.740 5.064 0.9094 0.9215 0.9028 0.7441 0.5104 0.7693 Image 4 6.754 6.918 0.9352 0.9425 0.8823 0.7827 0.9463 Image 5 4.975 3.645 0.8502 0.9034 0.8808 0.7772 0.9104 0.7693 Image 6 5.118 4.556 4.978 0.8502 0.9034 0.8808 0.7772 0.9104 0	The part HE CACHE [2] SRIE [4] DRHT [8] Proposed The part HE CACHE [2] The part The part	Name	Name	

image. Figure 4 shows that the proposed method and SRIE produced high-quality images without banding artifacts. In contrast, images enhanced by HE and CACHE includes banding artifacts which are caused by quantized pixel values in the input image. This result denotes that the proposed method can restore lost pixel values due to the quantization.

Tables 1 and 2 illustrate results of objective assessment in terms of TMQI and NIQE. In case of TMQI, a larger value means a higher similarity between a target LDR image and an original HDR image. By contrast, a smaller value for NIQE indicates that a target LDR image has higher naturalness. As shown in Table 1, the proposed method provided the highest TMQI scores in the five methods for four images. HE also provided high TMQI scores, but HE cannot restore lost pixel values and it often causes the over-enhancement in bright areas. Moreover, as shown in Table 2, the proposed method also provided the best NIQE scores for six images (see Table 2). For these reasons, the proposed method outperforms the conventional methods in terms of both TMQI and NIQE.

Those experimental results show that the proposed method is effective for enhancing single images.

5. CONCLUSION

In this paper, a novel image enhancement network trained by using HDR images was proposed. The use of HDR images for training enables us to obtain higher-quality target images than that captured with cameras. Moreover, the proposed method has not only a higher performance but also a simpler network architecture, than the conventional CNN based method. Experimental results showed that the proposed method outperforms state-of-the-art conventional image enhancement methods in terms of TMQI and NIQE. In addition, visual comparison results demonstrated that the proposed method can restore lost pixel values, although conventional methods cannot. Because of space limitations, we have showed results for eight images, but the similar trend was confirmed for other images.

6. REFERENCES

- [1] K. Zuiderveld, *Contrast Limited Adaptive Histogram Equalization*. Elsevier, 1994, pp. 474–485.
- [2] X. Wu, X. Liu, K. Hiramatsu, and K. Kashino, "Contrast-accumulated histogram equalization for image enhancement," in 2017 International Conference on Image Processing (ICIP). IEEE, 2017, pp. 3190–3194.
- [3] X. Guo, Y. Li, and H. Ling, "LIME: Low-light image enhancement via illumination map estimation," *IEEE Transactions on Image Processing*, vol. 26, no. 2, pp. 982–993, Feb 2017.
- [4] X. Fu, D. Zeng, Y. Huang, X.-P. Zhang, and X. Ding, "A weighted variational model for simultaneous reflectance and illumination estimation," in *The IEEE Conference on Computer Vision and Pattern Recognition (CVPR)*, June 2016.
- [5] Y. Kinoshita, T. Yoshida, S. Shiota, and H. Kiya, "Pseudo multi-exposure fusion using a single image," in APSIPA Annual Summit and Conference, 2017, pp. 263–269.
- [6] Y. Kinoshita, S. Shiota, and H. Kiya, "A pseudo multiexposure fusion method using single image," *IEICE Transactions on Fundamentals of Electronics, Communications and Computer Sciences*, vol. 101, no. 11, pp. 1–9, 2018, (available on arXiv:1808.00195).
- [7] C. Chen, Q. Chen, J. Xu, and V. Koltun, "Learning to see in the dark," in 2018 Conference on Computer Vision and Pattern Recognition (CVPR). IEEE, 2018.
- [8] X. Yang, K. Xu, Y. Song, Q. Zhang, X. Wei, and R. W. Lau, "Image correction via deep reciprocating hdr transformation," in *Proceedings of the IEEE Conference on Computer Vision and Pattern Recognition*, 2018, pp. 1798–1807.
- [9] G. Eilertsen, J. Kronander, G. Denes, R. Mantiuk, and J. Unger, "HDR image reconstruction from a single exposure using deep CNNs," ACM Transactions on Graphics (TOG), vol. 36, no. 6, pp. 178:1–178:15, 2017.
- [10] Y. Kinoshita, S. Shiota, and H. Kiya, "Fast inverse tone mapping with reinhard's grobal operator," in 2017 IEEE International Conference on Acoustics, Speech and Signal Processing (ICASSP). IEEE, 2017, pp. 1972–1976.
- [11] E. Reinhard, M. Stark, P. Shirley, and J. Ferwerda, "Photographic tone reproduction for digital images," *ACM Transactions on Graphics (TOG)*, vol. 21, no. 3, pp. 267–276, 2002.
- [12] T. Murofushi, M. Iwahashi, and H. Kiya, "An integer tone mapping operation for hdr images expressed in floating point data," in 2013 IEEE International Conference on Acoustics, Speech and Signal Processing (ICASSP). IEEE, 2013, pp. 2479–2483.
- [13] E. H. Land, "The retinex theory of color vision," *Scientific american*, vol. 237, no. 6, pp. 108–129, 1977.

- [14] O. Ronneberger, P.Fischer, and T. Brox, "Unet: Convolutional networks for biomedical image segmentation," in *Medical Image Computing and Computer-Assisted Intervention (MICCAI)*, ser. LNCS, vol. 9351. Springer, 2015, pp. 234–241, (available on arXiv:1505.04597 [cs.CV]). [Online]. Available: http://lmb.informatik.uni-freiburg.de/Publications/2015/RFB15a
- [15] X. Glorot, A. Bordes, and Y. Bengio, "Deep sparse rectifier neural networks," in *Proceedings of the fourteenth international conference on artificial intelligence and statistics*, 2011, pp. 315–323.
- [16] S. Ioffe and C. Szegedy, "Batch normalization: Accelerating deep network training by reducing internal covariate shift," *arXiv preprint arXiv:1502.03167*, pp. 1–11, 2015.
- [17] "Github openexr." [Online]. Available: https://github.com/openexr/
- [18] "High dynamic range image examples." [Online]. Available: http://www.anyhere.com/gward/hdrenc/pages/originals.html
- [19] "The HDR photographic survey." [Online]. Available: http://rit-mcsl.org/fairchild/HDRPS/HDRthumbs.html
- [20] "EMPA HDR images dataset," this dataset is unavailable now. [Online]. Available: http://empamedia.ethz.ch/hdrdatabase/index.php
- [21] H. Nemoto, P. Korshunov, P. Hanhart, and T. Ebrahimi, "Visual attention in LDR and HDR images," in 9th International Workshop on Video Processing and Quality Metrics for Consumer Electronics (VPQM), 2015, pp. 1–6. [Online]. Available: http://mmspg.epfl.ch/hdr-eye
- [22] "Max planck institut informatik." [Online]. Available: http://resources.mpi-inf.mpg.de/hdr/gallery.html
- [23] K. He, X. Zhang, S. Ren, and J. Sun, "Delving deep into rectifiers: Surpassing human-level performance on imagenet classification," in *Proceedings of the IEEE in*ternational conference on computer vision, 2015, pp. 1026–1034.
- [24] D. P. Kingma and J. Ba, "Adam: A method for stochastic optimization," *arXiv preprint arXiv:1412.6980*, pp. 1–15, 2014.
- [25] H. Yeganeh and Z. Wang, "Objective quality assessment of tone mapped images," *IEEE Transactions on Image Processing*, vol. 22, no. 2, pp. 657–667, 2013.
- [26] A. Mittal, R. Soundararajan, and A. C. Bovik, "Making a completely blind image quality analyzer," *IEEE Signal Processing Letters*, vol. 20, no. 3, pp. 209–212, March 2013.